

Quantifying Fiber Tensile Contributions to Shear Strength in Fiber-Reinforced Clay

Akhila Palat

WSP New Zealand Ltd, Akhila.palat@wsp.com

Michael Thomson Hendry

Department of Civil and Environmental Engineering – University of Alberta, Canada

Mahya Roustaei

Department of Civil Engineering – Ghent University, Belgium

ABSTRACT: Understanding the strength of highly fibrous and fiber-reinforced soils remains a complex task despite extensive research. Triaxial compression tests reveal that these soils do not form a distinct shear plane but expand radially, raising questions about the validity of continued shearing. This behavior is largely due to tension within the fibers. This study is the first to illustrate how tensile stresses within fibers contribute to the overall shear strength of the composite. By conducting triaxial extension tests on fiber-reinforced clay, the study examines the effects of loading path, fiber length, fiber alignment, and effective confining pressure on undrained shear strength, excess pore water pressure, and mobilized fiber tension. A novel transparent fiber-reinforced soil was developed to observe fiber orientation within clay and understand the role of fiber orientation in influencing the tensile stresses mobilized within the fibers. Triaxial compression tests limited tensile stress mobilization within fibers, while triaxial extension tests showed stress values beyond the tension cut-off line. Longer fibers enhanced shear strength in extension tests but had an adverse effect in compression tests due to scale effects. Samples with vertically oriented fibers exhibited higher shear strength in extension tests, suggesting that the stiffest response occurs when the major principal stress is perpendicular to the fiber orientation. The paper further quantifies the tensile stresses in fiber-reinforced clays and demonstrates how these stresses are integrated into the soil's strength and failure mechanisms.

KEYWORDS: Fiber reinforcement, Shear strength, Pore pressure, Anisotropy, Tensile stresses, Triaxial extension.

1 INTRODUCTION

The incorporation of discrete fibers into soil matrices has emerged as a significant advancement in geotechnical engineering, offering enhanced mechanical properties and improved performance for various applications including hydraulic fill during land reclamation and deposition of fine tailings. Fiber reinforcement fundamentally alters the stress-strain behavior of soils by introducing tensile resistance through the fiber-matrix interface, creating a composite material with characteristics distinct from both the unreinforced soil and the reinforcing fibers individually.

Traditional geotechnical testing methods and strength evaluation approaches were developed for unreinforced soils and may not adequately capture the complex mechanisms governing fiber-reinforced soil behavior. Conventional consolidated undrained (CU) triaxial compression tests of fiber-reinforced clayey soils demonstrate several distinctive characteristics that challenge established interpretation methods: effective stress paths that approach the tension cut-off line, continuous strain hardening without well-defined peak shear stress, and the absence of clearly defined shear planes during failure. These behaviors are fundamentally attributed to the development of tension within the reinforcing fibers, which contributes to the overall strength of the composite material.

The mechanical response of fiber-reinforced soils is governed by the complex interaction between the soil matrix and the reinforcing elements. The reinforcement mechanism involves mobilization of tensile forces in the fibers, which are transferred to the soil matrix through interfacial shear stresses. This process results in a redistribution of stresses within the composite material, potentially leading to failure modes that differ significantly from those observed in unreinforced soils. However, the quantification of tensile stresses generated within fiber-reinforced soils and their incorporation into strength criteria remains poorly understood.

Current design approaches for fiber-reinforced soils often rely on empirical correlations or simplified analytical models that do not fully account for the tensile contribution of fibers to the overall strength. The development of appropriate failure criteria for fiber-reinforced soils requires a fundamental understanding of how tensile stresses manifest in the failure mechanism and how they can be reliably measured and quantified. This understanding is critical for advancing the design and application of fiber-reinforced soils in geotechnical engineering practice.

This study aims to investigate the fundamental mechanics of fiber-reinforced soils with particular emphasis on quantifying the tensile stresses generated within the composite material and understanding how these stresses influence the overall strength and failure mechanisms. The research focuses on developing a comprehensive understanding of the stress-strain behavior of fiber-reinforced clayey soils under various loading conditions, with the ultimate goal of establishing improved design criteria for fiber-reinforced soil applications in geotechnical engineering.

2 MATERIALS AND METHODS

2.1 *Materials*

The fine-grained soil used in this study is 'EPK Kaolin' manufactured by Edgar Minerals Inc. EPK Kaolin is adopted for testing considering its fine-grained texture and high permeability as reasonable estimates of pore water pressure can be measured during shearing. Additionally, the EPK Kaolin is a neutral material without any unique behavior and the material properties can be easily determined from basic laboratory testing. Laboratory testing of the soil gave a specific gravity of 2.45, liquid limit of 58%, plastic limit of 42%, plasticity index of 16%, Optimum moisture content (OMC) of 28%, and Maximum dry density (MDD) of 1.5 g/cm³.

The fibers used in this study are pre-cut polypropylene (PP) fibers supplied by MiniFIBERS Inc. (Johnson City, TN, USA). These fibers had a thickness of 0.035 mm, specific gravity of 0.91, tensile modulus of 0.4 GPa, and moisture absorption capacity less than 1% (as provided by the manufacturer). Synthetic fibers were selected for this study because their properties are controllable and pre-cut varieties of varying lengths can be easily procured from the manufacturer.

2.2 Sample preparation

To prepare unreinforced soil samples for testing, the required amount of dry kaolinite powder was mixed with distilled water (~145 mL) using an all-purpose wire whip mixer to form a slurry. This large quantity of water is required to avoid lumps in the kaolinite soil and ensure the slurry has a flowing consistency. A mixing time of 10 min was sufficient to obtain a homogeneous slurry. After mixing, the slurry was slowly poured into a cylindrical mold (150 mm diameter × 700 mm high) in layers to avoid the introduction of any air bubbles. Care was also taken to ensure no segregation while pouring the slurry. The slurry was allowed to self consolidate for 2 weeks at room temperature under the conditions of double drainage, followed by the application of incremental axial load up to a consolidation pressure of 100 kPa as this pressure was sufficient to obtain soil samples for testing. The block samples were then removed from the mold, covered with cling film, and stored in a moisture room until further testing. To prepare cylindrical samples for triaxial testing, a hollow round steel tube (50 mm diameter × 100 mm long) was pushed into the consolidated slurry block whereas a circular metal mold (63.5 mm diameter × 25 mm long) was used for obtaining samples for DS testing.

This same procedure was also adopted for preparing fiber-reinforced slurry samples, the only difference being that the dry kaolinite powder was initially mixed with the fibers before adding water. The large quantity of water added during mixing ensured that the fibers were uniformly distributed within the slurry and avoided the entangling of fibers in the blades of the mixer.

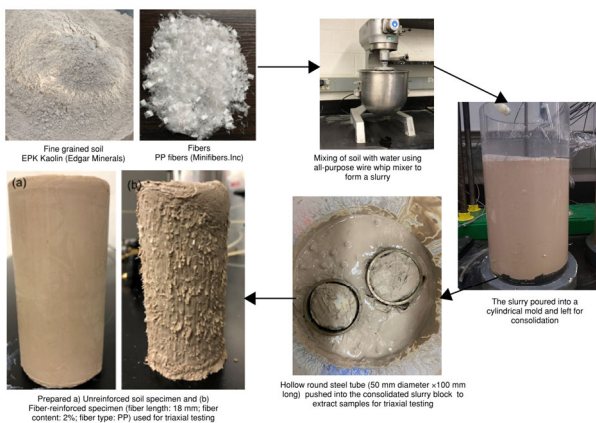


Figure 1. Methodology adopted for preparing unreinforced and fiber-reinforced samples for triaxial testing

2.3 Laboratory testing methodology

CU triaxial compression and extension tests were performed on unreinforced and fiber-reinforced samples to measure the undrained shear strength and excess pore water pressure developed within the composites. Both compression and extension tests were continued until an axial strain (ϵ_a) of 20% was obtained. Previous studies on fiber-reinforced fine-grained soils by Li (2005), Palat et al. (2019) and Correia et al., (2021) demonstrated that the load resisted by fibers is only substantial

at higher strain levels, hence small strain on-sample transducers were not employed in this testing. The strain rate for each of the triaxial tests was calculated based on the time required for 50% consolidation (t_{50}) in accordance with ASTM D4767-11 to ensure equalization of pore pressures throughout the specimen at failure.

2.3.1 CU triaxial compression tests

A Humboldt HM-5020 load frame with a capacity of 15 kN was used for performing CU triaxial compression tests on the samples, in accordance with ASTM D4767-11 (2020). A pressure panel was used to control the cell and back pressures applied to the sample. The pore water pressure developed within the specimen was measured by connecting a transducer at the base of the cell. The volume change in the sample during the consolidation phase was measured by attaching an automatic volume change device to the back pressure line of the triaxial chamber. The axial load was measured by a load cell (Model 75/1508, Sensotec) with a capacity of 4.5 kN and an accuracy of 0.14%. The vertical displacement of the sample was measured using a linear potentiometer (LP) (Model TR-50, Novotechnik) with a maximum travel length of 50 mm, linearity of $\pm 0.075\%$, and repeatability of ± 0.002 mm.

2.3.2 CU triaxial extension tests

A Bishop and Wesley stress path triaxial testing system was used to perform triaxial extension tests on the specimens. This testing system was accompanied with a multi-channel triaxial control and data acquisition software GEOSYS-Professional, both manufactured by Wille Geotechnik® (Götzenbreite, Germany). The samples were initially saturated by applying a cell pressure of 400 kPa and a backpressure of 390 kPa until Skempton's B parameter was greater than 0.97. The cell and back pressures were applied to the specimen using the automatic electro-mechanic volume/pressure controllers (VPC) with a capacity of 2 MPa, volume of 500 ml, and resolution of 0.1 kPa. The pore water pressure developed within the specimen was measured using a transducer connected to the base of the cell. Axial load was measured by a submersible load cell with a capacity of 10 kN and accuracy of 0.1%. The vertical displacement during shearing was measured by a linear variable differential transformer (LVDT) with a measuring range of 60 mm and resolution of 0.001 mm.

2.4 Scope of the testing program

An initial study evaluated fiber-reinforced fine-grained soil with fiber contents of 1%, 2%, and 3% (Palat and Hendry 2022). Results showed that deviator stress and pore water pressure peaked at 2% fiber content before declining at 3%, likely due to fiber clustering rather than uniform distribution. At higher fiber contents, shear among individual fibers becomes the governing factor, reducing overall shear strength. Therefore, all tests in this study used a constant 2% fiber content.

Table 1 lists the CU triaxial tests conducted as a part of this investigation. Each series included testing the triaxial specimens for three values of effective confining stresses (p'_0): 50, 100, and 200 kPa. The other variables used in this testing program are (1) loading path (compression and extension) and (2) fiber lengths (18 mm and 48 mm).

Table 1. Summary of the CU triaxial tests performed on unreinforced and fiber-reinforced soil as a part of this investigation.

| Type of specimen | Loading path | Fiber Length [mm] | p'_o [kPa] | Strain rate (%/minute) |
|------------------|--------------|-------------------|--------------|------------------------|
| Unreinforced | Extension | - | 50 | 0.7 |
| | | | 100 | 0.74 |
| | | | 200 | 0.76 |
| Unreinforced | Compression | - | 50 | 0.71 |
| | | | 100 | 0.73 |
| | | | 200 | 0.75 |
| Fiber-reinforced | Extension | 18 | 50 | 0.96 |
| | | | 100 | 1.02 |
| | | | 200 | 1.25 |
| Fiber-reinforced | Extension | 48 | 50 | 1.15 |
| | | | 100 | 1.3 |
| | | | 200 | 1.44 |
| Fiber-reinforced | Compression | 18 | 50 | 0.98 |
| | | | 100 | 1.04 |
| | | | 200 | 1.19 |
| Fiber-reinforced | Compression | 48 | 50 | 1.16 |
| | | | 100 | 1.26 |
| | | | 200 | 1.45 |

3 RESULTS AND DISCUSSIONS

3.1 Effect of fiber inclusion

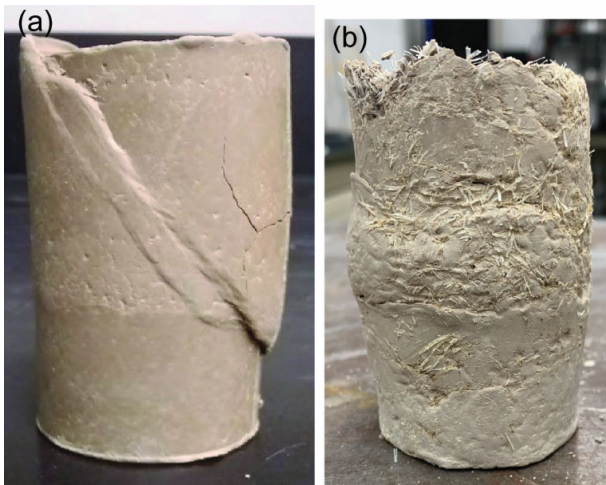


Figure 2. Deformation pattern in samples after failure when subjected to triaxial compression test: (a) unreinforced sample, (b) fiber-reinforced sample (fiber content: 2%; fiber length: 48 mm).

The effect of fiber inclusion was visually observed in all reinforced samples after shearing. The unreinforced clay samples failed at lower values of ϵ_a by developing a well-defined failure plane under compression and extension loading conditions (Figure 2a and Figure 3a). However, no visible failure plane was observed in the fiber-reinforced specimens after shearing. The fiber-reinforced samples showed a tendency to bulge in compression test (Fig. 2b); whereas an increase in length along with a reduction in diameter at the neck was observed in extension test (Fig. 3b). The testing was stopped once an ϵ_a of 20% was reached even though no visible failure was observed in the reinforced samples. This change in mode of failure could be visualized due to the movement of fibers to the potential plane of weakness and mobilization of tensile stresses within them (Palat et al., 2019; Palat and Hendry, 2021, 2022). Previous studies on compacted fiber-reinforced soils also observed a bulging behavior for the reinforced specimens and this change in the mode of failure was tied to the

improvement in the ductility of the soil by the addition of fibers (Freilich et al., 2017; Mirzababaei et al. 2017, 2018).

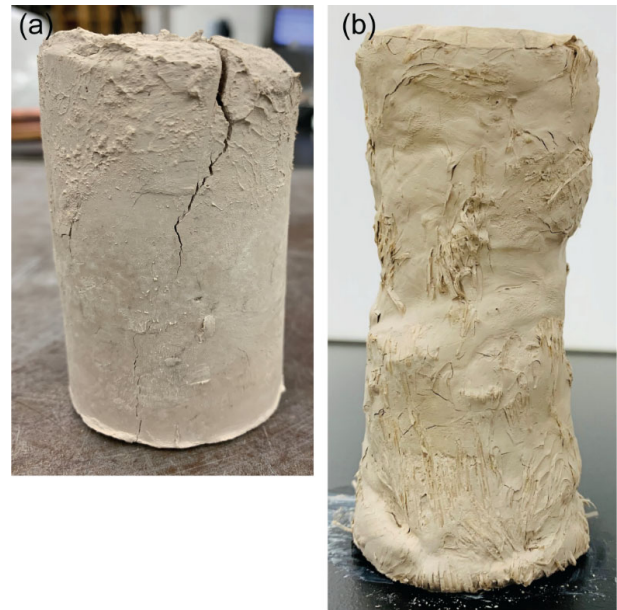


Figure 3. Deformation pattern in samples after failure when subjected to triaxial extension test: (a) unreinforced sample, (b) fiber-reinforced sample (fiber content: 2%; fiber length: 48 mm).

3.2 Effect of loading path

The plots in Figure 4 and Figure 5 summarize the effect of adding fibers of length 18 mm and 48 mm to a fine-grained soil subjected to triaxial compression and extension loading conditions respectively. The results are presented in terms of effective stress paths (ESPs) in deviator stress (q) versus mean effective stress (p'), q versus ϵ_a , and induced pore water pressure (Δu) versus ϵ_a .

In compression tests of 18 mm long fiber-reinforced composites, the ESP approaches the tension cut-off (TC) line and later follows the line (Fig. 4a) once the Δu developed within the composite becomes equal to the p'_o at which the specimen was sheared (Fig. 4c). Increasing the fiber length to 48 mm has a detrimental effect on the q and Δu values in compression test (Fig. 4b and 4c). On the contrary, the results from previous CU triaxial compression tests performed by the authors (Palat and Hendry, 2021, 2022) observed an increase in the q and Δu values with increasing fiber length when the fiber-reinforced samples were prepared by compacting. The reduced values of q and Δu observed in 48 mm long fiber-reinforced samples when prepared hydraulically using the slurry method is expected due to the increased tendency of 48 mm long fibers to be bent and twisted inside a 50 mm diameter Shelby tube thereby restricting the amount of tension mobilized within the fibers during shearing.

The mobilization of tensile stresses within the discrete fibers during shearing has been clearly demonstrated by performing a series of triaxial extension tests on the fiber-reinforced soil. The undrained ESP for all fiber-reinforced samples cross the TC line during shearing (Figs. 5a) and any increase in the q value beyond TC line is solely due to the tensile stresses developed within the fibers (Wood, 1990). Greater amount of tensile stress is mobilized in fibers of longer length and subsequently soil reinforced with 48 mm long fibers demonstrated higher values of q and Δu during shearing (Figs. 5b and 5c).

The TC line extending from the origin has a slope of 3:1 in the compression stress space (Fig. 4a) and -2:3 in the extension stress space (Fig. 5a). The TC line defines a limiting condition in the triaxial test where the soil can withstand no tensile effective stresses (Wood 1990). It represents zero effective radial stress in a triaxial compression test and zero effective axial stress in a triaxial extension test (Wood 1990). Thus any shear stress in excess of this line is solely due to tension within the specimen. Once shearing is initiated on the fiber-reinforced soil, tensile stress mobilizes within the fibers increasing the q and Δu developed within the composite (Palat and Hendry 2021). The undrained ESPs for the fiber-reinforced samples deviate to the left with a negative slope on further shearing. When the undrained ESP's approaches the TC line, $\sigma'_3 = 0$ with the value of Δu equals minor principal stress (σ_3).

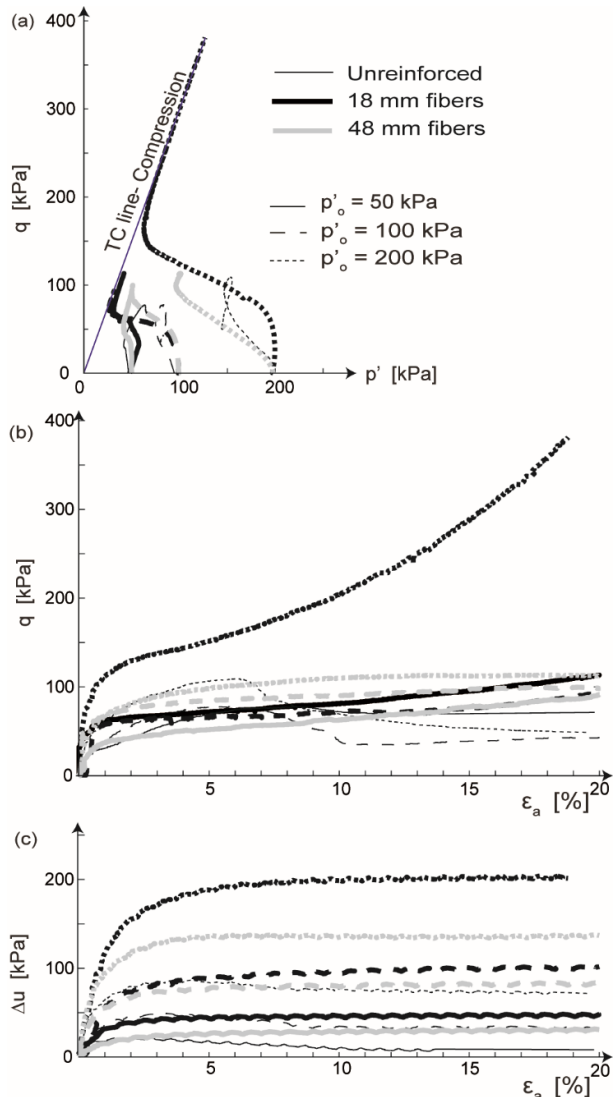


Figure 4. Comparison of CU compression testing results from unreinforced and fiber-reinforced specimens reinforced with 18 mm and 48 mm long fibers (fiber content: 2%; fiber type: PP) presented in (a) q versus p' space (b) q versus ϵ_a space, and (c) Δu versus ϵ_a space, at three values of p'_o .

For triaxial compression tests performed on 18 mm long fiber-reinforced soil (Fig. 4a) as well as for remoulded peat fibre specimens presented by Hendry et al. (2012), the portion of ESP corresponding to the linear strain hardening portion of the q versus ϵ_a curves traversed the TC line once Δu equals σ_3 . For

the ESP to cross the TC line, Δu developed within the soil has to exceed σ_3 . In a triaxial compression test, the σ_3 is the cell pressure (σ_{cell}). For the Δu to exceed the σ_{cell} in a compression test, water has to drain out from the specimen and none of the tests performed on fibrous soils were able to result in a tensile stress state. Subsequently, no previous tests on fibrous soils were able to demonstrate the mobilization of tensile stresses within the fibers during shearing and their contribution to the overall shear strength of the composite. This is an observed limitation of the use of CU triaxial compression tests in measuring the impacts of tensile elements within a soil. Attempts have been made in the past to define a strength for fibrous peat based on the onset of yielding within the measured response (Hendry et al. 2012, 2014). These shear strengths are conservative, discount the fiber reinforcement, and are often exceeded in practice without detriment.

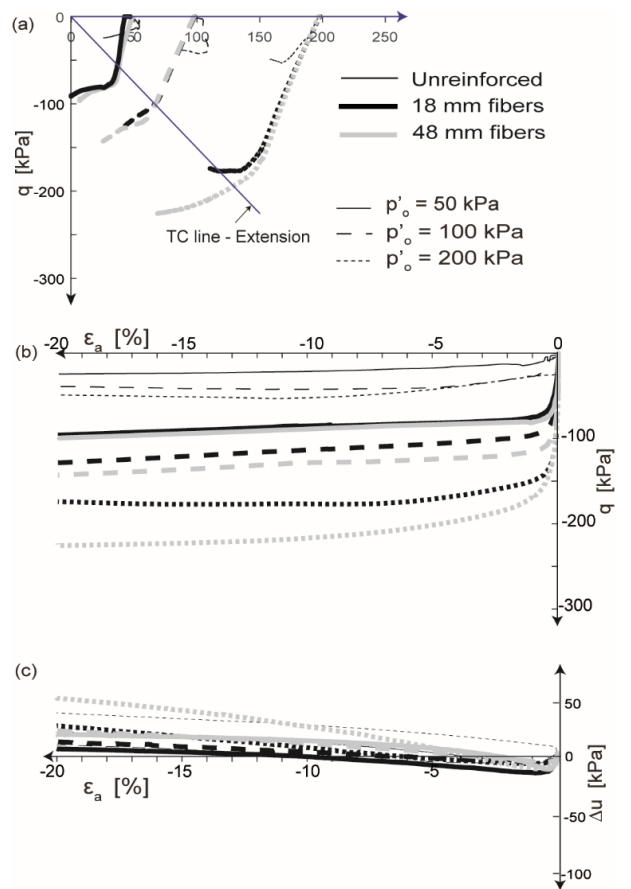


Figure 5. Comparison of CU extension testing results from unreinforced and fiber-reinforced specimens reinforced with 18 mm and 48 mm long fibers (fiber content: 2%; fiber type: PP) presented in (a) q versus p' space (b) q versus ϵ_a space, and (c) Δu versus ϵ_a space, at three values of p'_o .

The development of tensile stresses within the fibers has been demonstrated by performing a series of triaxial extension tests on fiber-reinforced clays. Any increase in the observed value of q beyond the TC line is only due to the tensile stresses mobilized in the fibers (Fig. 5a). This was possible because σ_3 acts in the axial direction for extension tests, and the condition of $\Delta u > \sigma_3$ can be attained while maintaining $\Delta u < \sigma_{cell}$, and thus preventing the drainage out of the specimen. The triaxial extension testing method imposes no restriction on the amount of tension mobilized within the fibers during undrained shearing. Higher values of q were observed in extension tests,

especially for samples reinforced with 48 mm long fibers due to the increased amount of tensile stresses mobilized within the fibers.

3.3 Effect of fiber length

For samples subjected to extension tests, the q and Δu developed within the composite increased with an increase in the length of fibers (Figs. 5b and 5c). This is expected due to two factors. Increasing the length of fiber augments the area of contact between fibers and soil leading to an increase in the interphase frictional component of shear strength. Additionally, increasing the fiber length improves the pullout resistance of individual fibers. This in turn leads to the mobilization of tensile stresses within the fibers, which contributes to the overall shear strength of the composite (Zornberg et al. 2004; Palat and Hendry, 2022).

On the other hand, greater amount of q and Δu was observed for 18 mm long fiber-reinforced composites subjected to triaxial compression tests. The ESP for 18 mm samples deviated to the left and approached the TC line. Increasing the fiber length to 48 mm reduced the q and Δu values developed within the fiber-reinforced clays. The inability of the ESP of 48 mm long fiber-reinforced clays to approach the TC line further states the reduction in the amount of tension mobilized in 48 mm long fibers. This is expected due to the tendency of 48 mm long fibers to bend and twist within a 50 mm diameter Shelby tube used for extracting fiber-reinforced samples for testing from the consolidated slurry. The bending of the fibers limits the amount of tension mobilized in the fibers during shearing, reducing the overall shear strength of the composite. The authors expect these bent 48 mm long fibers to untwine when subjected to extension tests and mobilize tensile stresses.

The primary objective of this study is to analyze the behavior of fibers when mixed hydraulically within a fine-grained soil with the intent of recommending this technique for the stabilization of mine fine tailings. The reduction in the values of q and Δu observed in the compression tests with increasing fiber length are expected due to the entanglement of 48 mm long fibers within a 50 mm diameter specimen. These boundary restrictions come because of triaxial sample preparation and are not expected to limit the amount of tensile stress mobilized within longer fibers while used for practical applications in the field. It is also recommended to perform further tests on larger diameter samples and confirm the influence of increasing fiber lengths on the q and Δu values developed in fiber-reinforced soils.

3.4 Stress distribution in fiber reinforced soil

In triaxial compression test, σ'_1 acts vertically and σ'_3 horizontally. When fiber – reinforced composites are subjected to triaxial compression test, the fibers within the sample align in the horizontal direction (perpendicular to the major principal stress, σ_1) during shearing and offer lateral resistance to the externally applied σ_a . In a triaxial compression test, σ'_t represents the lateral stress resisted by the fibers during shearing and it acts in the horizontal direction, opposite to the direction of expansive strain. The values of σ'_1 and σ'_3 acting on the fiber-reinforced soil subjected to a triaxial compression test is given in Equation (1) and Equation (2) respectively where σ'_a and σ'_r denote the effective axial and radial stress applied on the specimen.

$$\sigma'_1 = \sigma'_a + \sigma'_r \quad (1)$$

$$\sigma'_3 = \sigma'_r + \sigma'_t \quad (2)$$

In a triaxial extension test, the σ'_1 acts in the horizontal direction and σ'_3 acts in the vertical direction. When a fiber-reinforced soil is subjected to triaxial extension test, the fibers within the soil realign in the vertical direction (perpendicular to σ_1) during shearing, resists the σ_a applied on the soil, thereby restricting the formation of a shear plane. The σ'_t represents the axial stress resisted by the fibers and acts in the vertical direction, opposite to the direction of expansive strain. Equation (3) and Equation (4) represent the σ'_1 and σ'_3 acting on a fiber-reinforced specimen subjected to triaxial extension test.

$$\sigma'_1 = \sigma'_r \quad (3)$$

$$\sigma'_3 = \sigma'_r + \sigma'_t - \sigma'_a \quad (4)$$

3.5 Estimation of tensile stresses from triaxial testing data

Landva and La Rochelle (1983) evaluated the shear characteristics of Radforth peats and demonstrated that the peat fibers affect the geotechnical behavior of peat by providing an internal resistance to shear deformations in the triaxial mode of shear. This internal resistance offered by the fibers against deformation was considered as a function of the friction between the fibers (or between the fibers and the matrix) and the tensile strength of the fibers. According to Landva and La Rochelle (1983), even though the resistance induced by the fibers cannot be measured directly in peat specimens, the fiber contribution can be determined from the Mohr's circles if the shear strength without fibers is known.

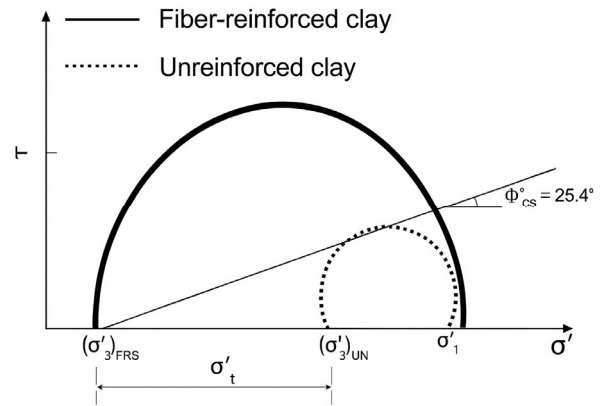


Figure 6. Conceptual representation of the stress resisted by the fibers during shearing (based on Landva and La Rochelle 1983)

Figure 6 represents the Mohr's circles for an unreinforced and fiber-reinforced soil subjected to the same value of σ'_1 . According to the conceptual model developed by Hendry et al (2014) for fibrous peat, the linear increase in q during strain hardening is the result of the shear resistance due to fiber tension. Hence, during the linear strain hardening response observed in the q versus ϵ_a curves of fiber-reinforced soil, the soil will be at its critical state. Direct shear tests performed as a part of this study estimated a ϕ'_{CS} of 25.4° for the soil. The value $(\sigma'_3)_{UN}$ can then be estimated from the applied values of σ'_1 and the ϕ'_{CS} of the soil from Equation 5.

$$(\sigma'_3)_{UN} = \frac{\sigma'_1}{\tan^2(45 + \frac{\phi'_{CS}}{2})} \quad (5)$$

The resulting shift to the left observed in the Mohr's circle of a fiber-reinforced soil corresponds to the resistance offered by the fibers during shearing (σ'_t). This value of σ'_t can then be estimated using Equation 6 where $(\sigma'_3)_{FRS}$ corresponds to σ'_3 acting on the fiber-reinforced soil as measured from the triaxial test.

$$\sigma'_T = (\sigma'_3)_{UN} - (\sigma'_3)_{FRS} \quad (6)$$

Following this procedure, the range of σ'_t generated in compression tests on specimens with horizontally oriented fibers was 15 to 152 kPa for 18 mm fibers and 5 to 45 kPa for 48 mm fibers. The range of σ'_t generated in extension tests on specimens with horizontally oriented fibers was 27 to 78 kPa for 18 mm fibers and 32 to 140 kPa for 48 mm fibers.

4 CONCLUSIONS

This study has provided fundamental insights into the mechanical behavior of fiber-reinforced clayey soils, with particular emphasis on quantifying tensile stresses within fibers during shearing. The investigation reveals key findings that advance our understanding of fiber-reinforced soil mechanics and their application in geotechnical engineering practice.

The most significant contribution is the successful demonstration and quantification of tensile stress mobilization within fiber-reinforced soils through triaxial extension testing. Unlike compression tests, which cannot achieve effective stress states beyond the tension cut-off line, extension tests measured the full fiber tension contributions ranging from 27 to 140 kPa depending on fiber length and orientation. The results of this study identify a limitation of current testing methodologies and establish that the loading path significantly influences mechanical response. In compression tests, fiber-reinforced specimens approach but cannot cross the tension cut-off line due to drainage restrictions. Conversely, extension tests allow effective stress paths to traverse this line, enabling direct measurement of fiber tensile contributions. This finding fundamentally challenges reliance on compression testing alone for characterizing fiber-reinforced soils.

From a practical standpoint, this research established a methodology for quantifying tensile stresses using conventional triaxial equipment. The proposed approach, based on Mohr circle analysis and critical state principles, provides a framework for incorporating fiber tension into strength calculations. The measured tensile stress values represent significant contributions previously underestimated in design practice.

This work contributes to the profession through methodological advancement by establishing extension testing as necessary for evaluating fiber-reinforced soils within a triaxial testing apparatus, quantitative framework development by providing first systematic quantification of tensile stresses under controlled conditions, mechanistic understanding by elucidating fundamental fiber-soil interaction mechanisms, design implications by demonstrating tensile contributions up to 140 kPa must be properly accounted for in calculations, and testing protocol enhancement by providing practical guidance for optimizing laboratory procedures. The research establishes a foundation for developing sophisticated constitutive models

that account for anisotropic fiber reinforcement and complex soil-fiber interactions. These advances are particularly relevant for mine tailings stabilization, hydraulic fills, and sustainable geotechnical solutions where fiber reinforcement offers significant advantages over traditional methods.

5 ACKNOWLEDGEMENTS

This research was funded by a Natural Sciences and Engineering Research Council Discovery Grant (RGPIN-2020-04419). The authors would also like to thank MiniFIBERS. Inc. for supplying the fibers for testing.

6 REFERENCES

- ASTM International. 2011. ASTM D4767-11: Standard Test Method for Consolidated Undrained Triaxial Compression Test for Cohesive Soils. ASTM International, West Conshohocken, PA.
- Correia, N.S., Rocha, S.A., Lodi, P.C., and McCartney, J.S. 2021. Shear strength behavior of clayey soil reinforced with polypropylene fibers under drained and undrained conditions. *Geotextiles and Geomembranes*, 49(5), 1419–1426.
- Freilich, B., Li, C., and Zornberg, J.G. 2010. Effective shear strength of fiber-reinforced clays. *Proceedings of the 9th International Conference on Geosynthetics, Geosynthetics 2009, São Paulo, Brazil, 1997–2000*.
- Hendry, M.T., Sharma, J.S., Martin, C.D., and Barbour, S.L. 2012. Effect of fibre content and structure on anisotropic elastic stiffness and shear strength of peat. *Canadian Geotechnical Journal*, 49(4), 403–415.
- Hendry, M.T., Barbour, S.L., and Martin, C.D. 2014. Evaluation of the effect of fibre reinforcement on the anisotropic undrained stiffness and strength of peat. *Journal of Geotechnical and Geoenvironmental Engineering*, 140(9).
- Landva, A.O., and La Rochelle, P. 1983. Compressibility and shear characteristics of Radforth peats. In: *Testing of Peats and Organic Soils*. ASTM STP 820, 157–191.
- Li, C. 2005. Mechanical response of fiber-reinforced soil. Ph.D. Thesis, University of Texas at Austin, Austin, TX.
- Mirzababaei, M., Mohamed, M., Arulrajah, A., Horpibulsuk, S., and Anggraini, V. 2017. Practical approach to predict the shear strength of fiber-reinforced clay. *Geosynthetics International*, 25(1).
- Mirzababaei, M., Arulrajah, A., Haque, A., Nimbalkar, S., and Mohajerani, A. 2018. Effect of fiber reinforcement on shear strength and void ratio of soft clay. *Geosynthetics International*, 25(4), 471–480.
- Palat, A., Hendry, M.T., and Roustaei, M. 2019. Effect of fiber content on the mechanical behavior of fiber-reinforced clay. *Proceedings of the 72nd Canadian Geotechnical Society Annual Conference, GeoStJohns 2019, St. John's, Newfoundland, 29 September–2 October 2019*.
- Palat, A., and Hendry, M.T. 2021. Evaluation of the geomechanical behavior of fiber-reinforced clay soil. *Proceedings of the 74th Canadian Geotechnical Society Annual Conference and the 14th Joint CGS/IAH-CNC Groundwater Conference, GeoNiagara 2021, Niagara Falls, Ontario, 26–29 September 2021*.
- Palat, A., and Hendry, M.T. 2022. Investigation of the behavior of fiber-reinforced clay soil. *Proceedings of the 20th International Conference on Soil Mechanics and Geotechnical Engineering (ICSMGE 2022), Sydney, Australia, 1–6 May 2022*.
- Wood, D.M. 1990. *Soil Behaviour and Critical State Soil Mechanics*. Cambridge University Press, Cambridge.
- Zornberg, J.G., Cabral, A.R., and Viratjandr, C. 2004. Behaviour of tire shred-sand mixtures. *Canadian Geotechnical Journal*, 41(2), 227–241.